

Saturation and Confinement: Analyticity, Unitarity and AdS/CFT Correspondence

Richard Brower¹, Marko Djuric², Chung-I Tan^{3†}

¹ Boston University, Boston, MA 02215, USA,

² Brown University, Providence, RI 02912, USA,

³ Brown University, Providence, RI 02912, USA.

DOI: <http://dx.doi.org/10.3204/DESY-PROC-2009-01/95>

Abstract

In $1/N_c$ expansion, analyticity and crossing lead to crossing even and odd ($C = \pm 1$) vacuum exchanges at high-energy, the *Pomeron* and the *Odderon*. We discuss how, using *String/Gauge duality*, these can be identified with a reggeized *Graviton* and the anti-symmetric *Kalb-Ramond fields* in *AdS* background. With confinement, these Regge singularities interpolate with glueball states. We also discuss unitarization based on eikonal sum in *AdS*.

1 Forward Scattering, Gauge/String Duality and Confinement

The subject of near-forward high energy scattering for hadrons has a long history. We focus here on the recent developments based on Maldacena's weak/strong duality, relating Yang-Mills theories to string theories in (deformed) Anti-de Sitter space [1–5]. For conformally invariant gauge theories, the metric of the dual string theory is a product, $AdS_5 \times W$, $ds^2 = \left(\frac{r^2}{R^2}\right) \eta_{\mu\nu} dx^\mu dx^\nu + \left(\frac{R^2}{r^2}\right) dr^2 + ds_W^2$, where $0 < r < \infty$. For the dual to $\mathcal{N} = 4$ supersymmetric Yang-Mills theory the AdS radius R is $R^2 \equiv \sqrt{\lambda} \alpha' = (g_{YM}^2 N)^{1/2} \alpha'$, and W is a 5-sphere of this same radius. We will ignore fluctuations over W and also assume that $\lambda \gg 1$, so that the spacetime curvature is small on the string scale, and $g_{YM}^2 \ll 1$ so that we can use string perturbation theory. (See [3, 4] for more references.)

The fact that 5-dim description enters in high energy collision can be understood as follows. In addition to the usual LC momenta, $p_\pm = p^0 \pm p^z$ (2d), and transverse impact variables, \vec{b} (2d), there is one more “dimension”: a “resolution” scale specified by a probe, e.g., $1/Q^2$ of virtual photon in DIS, (see Fig. 1a.) Because of conformal symmetry, these 5 coordinates transform into each others, leaving the system invariant. In the strong coupling limit, conformal symmetry is realized as the $SL(2, C)$ isometries of Euclidean AdS_3 subspace of AdS_5 , where r can be identified with Q^2 .

The traditional description of high-energy small-angle scattering in QCD has two components — a soft Pomeron Regge pole associated with exchanging tensor glueballs, and a hard BFKL Pomeron at weak coupling. On the basis of gauge/string duality, a coherent treatment of the Pomeron was provided [1]. These results agree with expectations for the BFKL Pomeron at negative t , and with the expected glueball spectrum at positive t , but provide a framework in which they are unified [6].

One important step in formulating the dual Pomeron involves the demonstration [7] that in exclusive hadron scattering, the dual string theory amplitudes at wide angle, due to the red-shifted local-momenta, $s \rightarrow \tilde{s} = (R/r)^2 s$ and $t \rightarrow \tilde{t} = (R/r)^2 t$, give the power laws that are expected in a gauge

[†] speaker

theory. It was also noted that at large s and small t that the classic Regge form of the scattering amplitude should be present in certain kinematic regimes [7, 8]. Equally important is the fact that, with confinement, transverse fluctuations of the metric tensor G_{MN} in AdS acquire a mass and can be identified with a tensor glueball [9, 10]. It was suggested in [10] that, at finite λ , this will lead to a Pomeron with an intercept below 2. That is, Pomeron can be considered as a *Reggeized Massive Graviton*.

The *dual Pomeron* was subsequently identified as a well-defined feature of the curved-space string theory [1]. For a conformal theory in the large N_c limit, a dual Pomeron can always be identified with the leading eigenvalue of a Lorentz boost generator M_{+-} of the conformal group [3]. The problem reduces to finding the spectrum of a single J -plane Schrödinger operator. In the strong coupling limit, conformal symmetry requires that the leading $C = +1$ Regge singularity is a fixed J -plane cut. For ultraviolet-conformal theories with confinement deformation, the spectrum exhibits a set of Regge trajectories at positive t , and a leading J -plane cut for negative t , the cross-over point being model-dependent. (See Fig. 1b.) For theories with logarithmically-running couplings, one instead finds a discrete spectrum of poles at all t , with a set of slowly-varying and closely-spaced poles at negative t .

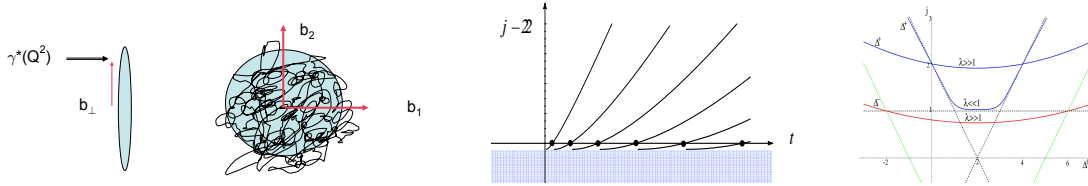


Fig. 1: (a) Intuitive picture for AdS^5 kinematics. (b) Schematic representation of J -plane singularity structure. (c) Schematic form of Δ - j relation for $\lambda \ll 1$ and $\lambda \gg 1$ for $C = +1$ and $\lambda \gg 1$ for $C = -1$.

2 Conformal Pomeron, Odderon and Analyticity

At high-energy, analyticity and crossing lead to $C = \pm 1$ vacuum exchanges, the *Pomeron* and the *Odderon*. The qualitative picture for Pomeron exchange in weak coupling [11] has been understood for a long time, in leading order expansion in g_{YM}^2 and all order sum in $g_{YM}^2 \log(s/s_0)$. In the conformal limit, both the weak-coupling BFKL Pomeron and Odderons correspond to J -plane branch points, e.g., the BFKL Pomeron is a cut at $j_0^{(+)}$, above $j = 1$. Two leading Odderons have been identified. (See [4, 12] for more references.) Both are branch cuts in the J -plane. One has an intercept slightly below 1 [13], and the second has an intercept precisely at 1 [14]. These are summarized in Table 1.

In the strong coupling limit, conformal symmetry dictates that the leading $C = +1$ Regge singularity is a fixed J -plane cut at $j_0^{(+)} = 2 - 2/\sqrt{\lambda} + O(1/\lambda)$. As λ increases, the “conformal Pomeron” moves to $j = 2$ from below, approaching the AdS graviton. We have recently shown [4] that the strong coupling *conformal odderons* are again fixed cuts in the J -plane, with intercepts specified by the AdS mass squared, m_{AdS}^2 , for Kalb-Ramond fields [15],

$$j_0^{(-)} = 1 - m_{AdS}^2/2\sqrt{\lambda} + O(1/\lambda). \quad (1)$$

Interestingly, two leading *dual odderons* can be identified, parallel the weak-coupling situation. One solution has $m_{AdS,(1)}^2 = 16$. There is also a second solution where $m_{AdS,(2)}^2 = 0$. We outline below how these features emerge in *Gauge/String duality*.

	Weak Coupling	Strong Coupling
$C = +1$: Pomeron	$j_0^{(+)} = 1 + (\ln 2) \lambda/\pi^2 + O(\lambda^2)$	$j_0^{(+)} = 2 - 2/\sqrt{\lambda} + O(1/\lambda)$
$C = -1$: Odderon	$j_{0,(1)}^{(-)} \simeq 1 - 0.24717 \lambda/\pi + O(\lambda^2)$ $j_{0,(2)}^{(-)} = 1 + O(\lambda^3)$	$j_{0,(1)}^{(-)} = 1 - 8/\sqrt{\lambda} + O(1/\lambda)$ $j_{0,(2)}^{(-)} = 1 + O(1/\lambda)$

Table 1: Pomeron and Odderon intercepts at weak and strong coupling, with $\lambda = g_{YM}^2 N_c$ the 't Hooft coupling.

2.1 Flat-Space Expectation for $C = \pm 1$ Sectors

String scattering in 10-d flat-space at high energy leads to a crossing-even and crossing-odd amplitudes,

$$\mathcal{T}_{10}^{(\pm)}(s, t) \rightarrow f^{(\pm)}(\alpha' t) (\alpha' s)^{\alpha_{\pm}(t)}, \quad (2)$$

where $\alpha_+(t) = 2 + \alpha' t/2$ and $\alpha_-(t) = 1 + \alpha' t/2$ respectively. That is, at $t = 0$, a massless state with integral spin is being exchanged, e.g., for $C = +1$, one is exchanging a massless spin-2 particle, the ubiquitous graviton. Of course, the coefficient functions, $f^{(\pm)}(\alpha' t)$, are process-dependent.

Massless modes of a closed string theory can be identified with transverse fluctuations coming from a left-moving and a right-moving level-one oscillators, e.g., states created by applying $a_{1,J}^\dagger \tilde{a}_{1,J}^\dagger$ to the vacuum, i.e., $a_{1,J}^\dagger \tilde{a}_{1,J}^\dagger |0; k^+, k_\perp\rangle$, with $k^2 = 0$. Since a 10-dim closed string theory in the low-energy limit becomes 10-dim gravity; these modes can be identified with fluctuations of the metric G_{MN} , the anti-symmetric Kalb-Ramond background B_{MN} [15], and the dilaton, ϕ , respectively. It is important to note that we will soon focus on AdS^5 , i.e., one is effectively working at $D = 5$. With $D = 5$, the independent components for G_{MN} and B_{MN} are 5 and 3 respectively, precisely that necessary for having (massive) states with spin 2 and 1 [10]. For oriented strings, it can be shown that the symmetric tensor contributes to $C = +1$ and the anti-symmetric tensor contributes to $C = -1$.

2.2 Diffusion in AdS for Pomeron and Odderon

Let us next introduce diffusion in AdS. We will restrict ourselves to the conformal limit. Regge behavior is intrinsically non-local in the transverse space. For flat-space scattering in 4-dimension, the transverse space is the 2-dimensional impact parameter space, \vec{b} . In the Regge limit of s large and $t < 0$, the momentum transfer is transverse. Going to the \vec{b} -space, $t \rightarrow \nabla_b^2$, and the flat-space Regge propagator, for both $C = \pm 1$ sectors, is nothing but a diffusion kernel, $\langle \vec{b} | (\alpha' s)^{\alpha_{\pm}(0) + \alpha' t \nabla_b^2/2} | \vec{b}' \rangle$, with $\alpha_+(0) = 2$ and $\alpha_-(0) = 1$ respectively. In moving to a ten-dimensional momentum transfer \tilde{t} , we must keep a term coming from the momentum transfer in the six transverse directions. This extra term leads to diffusion in extra-directions, i.e., for $C = +1$, $\alpha' \tilde{t} \rightarrow \alpha' \Delta_P \equiv \frac{\alpha' R^2}{r^2} \nabla_b^2 + \alpha' \Delta_{\perp P}$. The transverse Laplacian is proportional to R^{-2} , so that the added term is indeed of order $\alpha'/R^2 = 1/\sqrt{\lambda}$. To obtain the $C = +1$ Regge exponents we will have to diagonalize the differential operator Δ_P . Using a Mellin transform, $\int_0^\infty d\tilde{s} \tilde{s}^{-j-1}$, the Regge propagator can be expressed as $\tilde{s}^{2 + \alpha' \tilde{t}/2} = \int \frac{dj}{2\pi i} \tilde{s}^j G^{(+)}(j) = \int \frac{dj}{2\pi i} \frac{\tilde{s}^j}{j - 2 - \alpha' \Delta_P/2}$ where $\Delta_P \simeq \Delta_j$, the tensorial Laplacian. Using a spectral analysis, it leads to a J -plane cut at $j_0^{(+)}$.

A similar analysis can next be carried out for the $C = -1$ sector. We simply replace the Regge kernel by $\tilde{s}^{1+\alpha' i/2} = \int \frac{dj}{2\pi i} \tilde{s}^j G^{(-)}(j) = \int \frac{dj}{2\pi i} \tilde{s}^j (j - 1 - \alpha' \Delta_O/2)^{-1}$. The operator $\Delta_O(j)$ can be fixed by examining the EOM at $j = 1$ for the associated super-gravity fluctuations responsible for this exchange, i.e., the anti-symmetric Kalb-Ramond fields, B_{MN} . One finds two solutions,

$$G^{(-)}(j) = \frac{1}{[j - 1 - (\alpha'/2R^2)(\square_{Maxwell} - m_{AdS,i}^2)]}, \quad (3)$$

$i = 1, 2$, where $\square_{Maxwell}$ stands for the Maxwell operator. Two allowed values are $m_{AdS,1}^2 = 16$ and $m_{AdS,2}^2 = 0$. A standard spectral analysis then lead to a branch-cut at $j_0^{(-)}$, given by Eq. (1).

2.3 Regge and DGLAP Connection

It is also useful to explore the conformal invariance as the isometry of transverse AdS_3 . Upon taking a two-dimensional Fourier transform with respect to q_\perp , where $t = -q_\perp^2$, one finds that $G^{(\pm)}$ can be expressed simply as

$$G^{(\pm)}(z, x^\perp, z', x'^\perp; j) = \frac{1}{4\pi z z'} \frac{e^{(2-\Delta^{(\pm)}(j))\xi}}{\sinh \xi}, \quad (4)$$

where $\cosh \xi = 1 + v$, $v = [(x^\perp - x'^\perp)^2 + (z - z')^2]/(2zz')$ the AdS_3 chordal distance, and $z = R^2/r$, and $\Delta^{(\pm)}(j) = 2 + \sqrt{2} \lambda^{1/4} \sqrt{(j - j_0^{(\pm)})}$ is a J -dependent effective AdS_5 conformal dimension [1,3,4]. The $\Delta - j$ curve for $\Delta^{(\pm)}$ is shown in Fig. 1c. A related discussion on $\Delta(j)$ can be found in [16].

For completeness, we note that, for both $C = +1$ and $C = -1$, it is useful to introduce Pomeron and Odderon kernels in a mixed-representation,

$$\mathcal{K}^{(\pm)}(s, z, x^\perp, z', x'^\perp) \sim \left(\frac{(zz')^2}{R^4} \right) \int \frac{dj}{2\pi i} \left[\frac{(-\tilde{s})^j \pm (\tilde{s})^j}{\sin \pi j} \right] G^{(\pm)}(z, x^\perp, z', x'^\perp; j). \quad (5)$$

To obtain scattering amplitudes, we simply fold these kernels with external wave functions. Eq. (5) also serves as the starting point for eikonalization.

3 Unitarity, Absorption, Saturation and the Eikonal Sum

For simplicity, we will focus here on the $C = +1$ sector, assuming all crossing odd amplitudes vanish. It has been shown in Refs. [?, 2, 3] that, in the strong coupling limit, a 2-to-2 amplitude, $A(s, t)$, in the near-forward limit can be expressed in terms of a ‘‘generalized’’ eikonal representation,

$$A_{2 \rightarrow 2}(s, t) = \int dz dz' P_{13}(z) P_{24}(z') \int d^2 b e^{-ib^\perp q_\perp} \tilde{A}(s, b^\perp, z, z'), \quad (6)$$

where $\tilde{A}(s, b^\perp, z, z') = 2is \left[1 - e^{i\chi(s, b^\perp, z, z')} \right]$, and $b^\perp = x^\perp - x'^\perp$ due to translational invariance. The probability distributions for left-moving, $P_{13}(z)$, and right moving, $P_{14}(z)$ particles are products of initial (in) and final (out) particle wave functions. The eikonal, χ , can be related to the strong coupling Pomeron kernel [1, 3], and can be expressed as the inverse Mellin transform of $G^{(+)}(j, x^\perp - x'^\perp, z, z')$.

We note the salient feature of eikonal scattering locally in transverse AdS_3 , and the near-forward field-theoretic amplitude is obtained from a bulk eikonal amplitude after convolution. It is useful to

focus our attention on the properties of the bulk eikonal formula $\tilde{A}(s, b^\perp, z, z')$ itself. For χ real, it is elastic unitary. On the other hand, when χ is complex, (with $\text{Im}\chi > 0$), one has inelastic production. Absorption and saturation can now be addressed in this context. It is also important to note that, for Froissart bound, confinement is crucial. Discussion on these and related issues can be found in Ref. [3].

We end by pointing out one unique feature of strong coupling – the eikonal is predominantly real. To simplify the discussion, let us consider the second order contributions to the imaginary part of the elastic amplitude. The AGK cutting rule for the imaginary part of the elastic amplitude generalizes to

$$\cos(j_0\pi)|\chi|^2 = [1 - 2\sin^2(j_0\pi/2) - 2\sin^2(j_0\pi/2) + 2\sin^2(j_0\pi/2)] |\chi|^2 \quad (7)$$

where the first term on the right is due to the elastic scattering, the last term is due to two-cut-Pomeron contribution, and the second and the third are due to one-cut-Pomeron contributions. The tradition weak coupling approach to diffraction scattering has $j_0 \simeq 1$, leading to a net negative contribution: $-1 = 1 - 2 - 2 + 2$. This leads to absorption, already dominant at second order. However, for extreme strong coupling, one has $j_0 \simeq 2$, leading to a positive cut contribution: $1 = 1 - 0 - 0 + 0$. This is consistent with scattering being predominantly elastic. However, the real world is neither strictly weak coupling nor strong coupling. For $j_0 \simeq 1.5$, one finds the two-Pomeron contribution vanishes: $0 = 1 - 1 - 1 + 1$. That is, what used to be the dominant correction to elastic scattering now vanishes. Clearly, these issues deserve further examination. For applications of [1–5] for DIS, see [17].

References

- [1] R. C. Brower, J. Polchinski, M. J. Strassler, and C.-I. Tan, *JHEP* **12**, 005 (2007). [hep-th/0603115](#).
- [2] R. C. Brower, M. J. Strassler, and C.-I. Tan (2007). [arXiv:0707.2408 \[hep-th\]](#).
- [3] R. C. Brower, M. J. Strassler, and C.-I. Tan (2007). [0710.4378](#).
- [4] R. C. Brower, M. Djuric, and C.-I. Tan (2008). [0812.0354](#).
- [5] L. Cornalba, M. S. Costa, J. Penedones, and R. Schiappa (2007). [hep-th/0611122](#);
L. Cornalba, M. S. Costa, J. Penedones, and R. Schiappa, *Nucl. Phys.* **B767**, 327 (2007). [hep-th/0611123](#);
L. Cornalba, M. S. Costa, and J. Penedones (2007). [arXiv:0707.0120 \[hep-th\]](#).
- [6] E. Levin and C.-I. Tan, “Proc. for International Symposium on Multiparticle Dynamics”, Santiago, Spain, July 1992, and “Workshop on Small-x and Diffractive Physics at Tevatron”, FNAL, Sept. 1992 (1992). [hep-ph/9302308](#).
- [7] J. Polchinski and M. J. Strassler, *Phys. Rev. Lett.* **88**, 031601 (2002). [hep-th/0109174](#).
- [8] R. C. Brower and C.-I. Tan, *Nucl. Phys.* **B662**, 393 (2003). [hep-th/0207144](#).
- [9] R. C. Brower, S. D. Mathur, and C.-I. Tan, *Nucl. Phys.* **B574**, 219 (2000). [hep-th/9908196](#).
- [10] R. C. Brower, S. D. Mathur, and C.-I. Tan, *Nucl. Phys.* **B587**, 249 (2000). [hep-th/0003115](#).
- [11] L. N. Lipatov, *Sov. J. Nucl. Phys.* **23**, 338 (1976);
E. A. Kuraev, L. N. Lipatov, and V. S. Fadin, *Sov. Phys. JETP* **45**, 199 (1977);
I. I. Balitsky and L. N. Lipatov, *Sov. J. Nucl. Phys.* **28**, 822 (1978).
- [12] C. Ewerz (2005). [hep-ph/0511196](#).
- [13] R. A. Janik and J. Wosiek, *Phys. Rev. Lett.* **82**, 1092 (1999). [hep-th/9802100](#);
M. A. Braun (1998). [hep-ph/9805394](#).
- [14] J. Bartels, L. N. Lipatov, and G. P. Vacca, *Phys. Lett.* **B477**, 178 (2000). [hep-ph/9912423](#).
- [15] M. Kalb and P. Ramond, *Phys. Rev.* **D9**, 2273 (1974).
- [16] D. M. Hofman and J. Maldacena, *JHEP* **05**, 012 (2008). [0803.1467](#).
- [17] E. Levin, J. Miller, B. Z. Kopeliovich, and I. Schmidt (2008). [0811.3586](#);
Y. Hatta, E. Iancu, and A. H. Mueller (2007). [arXiv:0710.2148 \[hep-th\]](#);
L. Cornalba and M. S. Costa (2008). [0804.1562](#).